1 **Water availability limits tree productivity, carbon stocks, and carbon residence time in**

2 **mature forests across the western United States**

4 Logan T. Berner *[1], Beverly E. Law [1], and Tara W. Hudiburg [2]

6 [1] Department of Forest Ecosystems and Society

7 Oregon State University

8 321 Richardson Hall

9 Corvallis, Oregon 97331-2212

11 [2] Department of Forest, Rangeland, and Fire Sciences

12 University of Idaho

13 875 Perimeter Drive

14 Moscow, Idaho 83844-1133

16 * Corresponding Author:

17 logan.berner@oregonstate.edu

18 phone: 702-683-9987

19 fax: 541-737-5814

21 *Running header:*

22 Water limitations on forests in the western US

24 *Keywords:*

25 Bioclimatic gradient, carbon cycle, climate change, climate moisture index, forest inventory,

26 MODIS, satellite remote sensing, biomass

28 *Type of paper:*

29 Primary research article

31 **Abstract**

32 Water availability constrains the structure and function of terrestrial ecosystems and is projected

33 to change in many parts of the world over the coming century. We quantified the response of tree

34 net primary productivity (NPP), live biomass (BIO), and mean carbon residence time

35 (CRT=BIO/NPP) to spatial variation in water availability in the western US. We used forest

36 inventory measurements from 1,953 mature stands (>100 years) in Washington, Oregon, and

37 California (WAORCA) along with satellite and climate data sets covering the western US. We

38 summarized forest structure and function in both domains along a 400 cm yr^{-1} hydrologic

39 gradient, quantified with a climate moisture index (CMI) based on the difference between

40 precipitation and reference evapotranspiration summed over the water-year (October-September)

41 and then averaged annually from 1985-2014 ($CMI_{\overline{wy}}$). Median NPP, BIO, and CRT computed at

42 10 cm yr^{-1} intervals along the $CMI_{\overline{wy}}$ gradient increased monotonically with increasing $CMI_{\overline{wy}}$

43 across both WAORCA (r_s=0.93-0.96, p<0.001) and the western US (r_s=0.93-0.99, p<0.001).

44 Field measurements from WAORCA showed that median NPP increased from 2.2 to 5.6 Mg C

45 ha^{-1} yr^{-1} between the driest and wettest 5% of sites, while BIO increased from 26 to 281 Mg C

46 ha^{-1} and CRT increased from 11 to 49 years. The satellite data sets revealed similar changes over

47 the western US, though these data sets tended to plateau in the wettest areas, suggesting that

48 additional efforts are needed to better quantify NPP and BIO from satellites in high-productivity,

49 high-biomass forests. Our results illustrate that long-term average water availability is a key

50 environmental constraint on tree productivity, carbon storage, and carbon residence time in

51 mature forests across the western US, underscoring the need to assess potential ecosystem

52 response to projected warming and drying over the coming century.

53

1 Introduction

Water availability strongly constrains the distribution of plants on Earth's land surface (Holdridge, 1947; Major, 1963) and the resulting structure and function of terrestrial ecosystems (Churkina and Running, 1998; Law et al., 2002; Schuur, 2003). For instance, desert (Whittaker and Niering, 1975), grassland (Yang et al., 2008) and forest productivity (Law et al., 2002; Schuur, 2003; Berner and Law, 2015) differ widely among sites with contrasting water availability. Water availability is shaped by regional climate (e.g., precipitation, atmospheric evaporative demand), as well as by local topography and soils (Webb et al., 1983). Water availability is projected to change in many parts of the world over the coming century in response to continued atmospheric warming from sustained anthropogenic greenhouse gas emissions (Collins et al., 2013; Dai, 2013; Walsh et al., 2014). Societies depend on the goods and services provided by terrestrial ecosystems (e.g., forests; Williams, 2006) and thus it is imperative to elucidate climatic controls over ecosystem structure and function to help anticipate and mitigate potential impacts of ongoing climatic change.

The western United States is a region where pronounced spatial variation in water availability exerts a strong influence over forest structure and function. For instance, average annual precipitation varies over 500 cm yr^{-1} across this region, with particularly steep hydrologic gradients in the Pacific Northwest (Daly et al., 2008). Differences in water availability gives rise to forest communities that range from dry, low-productivity woodlands to high-productivity coastal temperate rainforests where live tree biomass (BIO) attains levels thought to be exceeded only by primary *Eucalyptus regnans* forests in southern Australia (Waring and Franklin, 1979; Keith et al., 2009).

76   Prior studies drew on small networks of field sites (n < 20) to investigate how tree net

77   primary productivity (NPP) and BIO varied among mature stands spread along hydrologic

78   gradients in parts of this region (Whittaker and Niering, 1975; Gholz, 1982; Webb et al., 1983;

79   Berner and Law, 2015). Tree BIO and NPP can vary widely with stand age (Hudiburg et al.,

80   2009) and thus these studies focused on mature stands (stand age generally > 100 years) where

81   BIO and NPP had somewhat stabilized after reaching their 'climatic potential.' These studies

82   showed that BIO and NPP tended to increase linearly or curvilinearly across sites as average

83   water availability increased (Whittaker and Niering, 1975; Gholz, 1982; Webb et al., 1983;

84   Berner and Law, 2015). These spatial relationships are thought to reflect long-term climatic

85   constraints on ecosystem structure (e.g., BIO) and function (e.g., NPP) that are shaped by

86   gradual shifts in community composition and population size (Jin and Goulden, 2014). The field

87   studies mentioned above make a compelling case that water availability is an important

88   determinant of BIO and NPP in mature stands, yet these studies were based on a small number of

89   field sites selected using a set of criteria (e.g., mature stands near a road) rather than on a large

90   sample of mature stands in the region.

91   Several of these earlier field studies also indicated that plant communities accumulated

92   more BIO per unit of NPP in progressively wetter areas, suggesting slower turnover of plant BIO

93   as climate became wetter (Whittaker and Niering, 1975; Webb et al., 1983). Mean carbon

94   residence time (CRT) describes the average duration that a carbon molecule will remain in a

95   specific pool (Waring and Running, 2007) and for CRT in live biomass can be computed as

96   BIO/NPP assuming that BIO remains constant over time (Whittaker, 1961; Friend et al., 2014).

97   CRT in live biomass is also known as the *biomass accumulation ratio* (Whittaker, 1961) and

98   ranged, for instance, from ~2 years in a hot desert shrubland to ~75 years in an wet, old-growth

99   Douglas-fir forest (Webb et al., 1983). Differences in CRT among plant communities with

100   contrasting climate are potentially associated with shifts in carbon allocation (e.g. short-lived

101   fine roots and foliage vs. long-lived stem wood) and disturbance regimes (Girardin et al., 2010).

102   Together, these field studies illustrate that forest structure and function are constrained by water

103   availability in parts of the western US; however, additional efforts are needed to assess these

104   relationships at larger scales across the region, particularly given that climate models project a

105   pronounced shift towards hotter, drier conditions over much of the region during the coming

106   century (Collins et al., 2013; Walsh et al., 2014; Cook et al., 2015).

107   Our objective in this study was to explore how forest structure and function change along

108   spatial gradients in water availability across the western US. We used the average water-year

109   climate moisture index ($CMI_{\overline{wy}}$; 1985-2014) as an indicator of long-term water availability

110   (Webb et al., 1983; Hogg and Hurdle, 1995), which we computed as the cumulative difference

111   between precipitation (P) and reference evapotranspiration (ET_0) over the approximate seasonal

112   cycle of soil water recharge and draw-down (October-September). Furthermore, we focused on

113   forest stands that were at least 100 years old because field surveys from the region indicated that

114   BIO and NPP reached much of their 'climatic potential' after a century, yet we acknowledge that

115   BIO tends to gradually increase and NPP remains stable or gradually declines during subsequent

116   centuries (Hudiburg et al., 2009). Building on prior field studies (e.g., Gholz, 1982; Webb et al.,

117   1983; Berner and Law, 2015), we hypothesized that long-term water availability limits tree NPP,

118   BIO, and CRT in mature forest stands across the region. We thus predicted that tree NPP, BIO,

119   and CRT in mature forests would increase with increasing $CMI_{\overline{wy}}$. Tree NPP, BIO, and CRT

120   were based on above- and below-ground components. We tested these hypotheses first across

121   Washington, Oregon, and California (WAORCA) using forest inventory measurements from

122   1,953 sites and then across 18 Mha of mature forest in the western US using satellite remote

123   sensing data sets. These data sets included three national biomass maps, along with NPP derived

124   from the Moderate Resolution Imaging Spectroradiometer (MODIS). Forest inventories provide

125   rigorous, though spatially-limited field measurements of forest structure and function, while

126   satellite remote sensing provides spatially-continuous, albeit modeled estimates of forest

127   structure and function across large domains.

128

2   Materials and methods

2.1   Data sets and preprocessing

2.1.1   Field estimates of tree biomass, productivity, and carbon residence time

132   We used field measurements to estimate BIO (BIO_{field}; Mg C ha^{-1}), NPP (NPP_{field}; Mg C ha^{-1} yr^{-1}

133   ^{1}), and CRT (CRT_{field}; year) at 1,953 forest inventory sites located in mature stands spread across

134   WAORCA. These 1-ha sites were surveyed by the US Forest Service Forest Inventory and

135   Analysis (FIA) program between 2001 to 2006 and comprise a representative sample of forest

136   lands (tree cover > 10%) in the region (Bechtold and Patterson, 2005). The inventory sites

137   occurred at elevations ranging from 5 m to 3,504 m, with an average (±1SD) elevation of

138   1429±677 m. We included sites in our analysis when stand age was at least 100 years. Stand age

139   was defined as the average age of the oldest 10% of trees, where individual tree age was

140   determined on survey plots using increment cores (Van Tuyl et al., 2005). BIO_{field} and NPP_{field}

141   were computed for each site as part of a prior study (Hudiburg et al., 2011). BIO_{field} was

142   estimated using regional allometric equations for tree components (e.g., stem, branch, bark,

143   foliage, and coarse roots) based on tree diameter and/or height (Means et al., 1994; Law et al.,

144   2001), along with estimates of fine root mass derived from a relationship with leaf area index

145   (LAI; m^2 leaf m^{-2} ground; Van Tuyl et al. 2005). NPP_{field} was estimated based on changes in

146   above- and below-ground woody biomass over a 10-year interval plus annual foliage and fine

147   root turn-over. See Hudiburg et al. (2011) for additional details. We then computed CRT_{field} in

148   live tree biomass as the ratio of BIO_{field} to $NPP_{field.}$

149

150   **2.1.2   Remote sensing estimates of tree biomass, productivity, and carbon residence time**

151   We used satellite remote sensing and ancillary data sets to estimate BIO (BIO_{sat}), NPP (NPP_{sat}),

152   and CRT (CRT_{sat}) across mature forests in the western US. BIO_{sat} included the same component

153   carbon pools as BIO_{field} (i.e, stem, branch, bark, foliage, coarse roots and fine roots). We

154   quantified the amount of carbon in stems, branches, and bark using an ensemble of three

155   satellite-derived data sets that depicted live tree aboveground biomass (AGB; excluded foliage)

156   circa 2000 to 2008 (Blackard et al., 2008; Kellndorfer et al., 2012; Wilson et al., 2013). Each

157   map was generated using satellite and geophysical (e.g., climate, topography) data sets to

158   spatially extrapolate forest inventory measurements over the conterminous US. We acquired

159   these maps at 250-m spatial resolution and then converted two of the maps (Blackard et al.,

160   2008; Kellndorfer et al., 2012) from dry biomass to carbon assuming a 50% conversion factor

161   (Smith et al., 2006). We then reprojected these maps onto a uniform grid in an equal area

162   projection, masked them to the common forest extent, and then averaged the AGB for each pixel

163   across the three biomass maps. We used the biomass map ensemble average in the subsequent

164   analysis, recognizing that pixel-wise estimates of AGC can vary notably among individual maps

165   (Neeti and Kennedy, 2016).

166   After deriving spatial estimates of carbon storage in AGB, we then estimated carbon

167   storage in coarse roots, fine roots, and foliage for each 250-m forested pixel. As with AGB, we

168   assumed that roots and foliage were 50% carbon (Smith et al., 2006; Berner and Law, 2016). We

169   computed coarse root biomass based on an empirical relationship with AGB (Cairns et al., 1997)

170   and fine root biomass based on an empirical relationship with peak summer LAI (Van Tuyl et al.,

171   2005). Spatial estimates of LAI were available globally at 1-km resolution from NASA's

172   Moderate Resolution Imaging Spectroradiometer (MODIS) as part of the MOD15A2 (Collection

173   5) data set (Myneni et al., 2002). We obtained these LAI estimates at 8-day intervals during July

174   and August (late-summer) from 2000 to 2014 for the western US. We then (1) excluded poor-

175   quality pixels using the quality control flags; (2) computed average late-summer LAI over the

176   15-year period; and (3) reprojected and resampled the data set to the common 250-m resolution

177   equal area grid. We used average late-summer MODIS LAI to computed both fine root biomass

178   (as described above) and foliage biomass. Foliage biomass was estimated for each pixel by

179   dividing LAI by the average specific leaf area (SLA; g C m^{-2} leaf) of the forest type found in that

180   pixel. We aggregated an existing map of forest type (Ruefenacht et al., 2008) into nine classes

181   (e.g., *Pinus ponderosa*, true fir) and then varied SLA among classes using species-, genus-, or

182   division-specific estimates of average SLA from a recent leaf trait synthesis (Berner and Law,

183   2016). We then estimated BIO_{sat} for each 250-m resolution pixel by summing the above- and

184   below-ground carbon pools.

185   We quantified regional NPP using the satellite-derived MODIS primary productivity data

186   set (NPP_{sat}; MOD17A3 v. 55). The MODIS light-use efficiency model predicts annual NPP at 1-

187 km resolution across global terrestrial ecosystems by incorporating estimates of absorbed

188 photosynthetically active radiation (APAR), LAI, and land cover derived from MODIS together

189 with plant physiological characteristics and climate data (Running et al., 2004; Zhao et al.,

190 2010). The model first predicts daily gross primary productivity (GPP) based APAR and the

191 efficiency with which APAR is converted to biomass (ϵ), which is affected by low temperatures

192 (frost) and high vapor pressure deficit (VPD) inducing stomatal closure. The model then

193 estimates plant respiration (R) at daily to annual increments and subsequently computes annual

194 NPP as the cumulative difference between GPP and R. These estimates thus reflect NPP

195 allocated both above- and below-ground. We acknowledge a degree of circularity in relating

196 NPP_{sat} to CMI given that both computations incorporate temperature data, specifically,

197 temperature-effects on VPD. We obtained annual NPP estimates from 2000 to 2014 for the

198 western US, reprojected the data onto an equal area grid, and then averaged over years.

199   Several additional preprocessing steps were required after deriving forest BIO_{sat} and

200 NPP_{sat}. These included masking both BIO_{sat} and NPP_{sat} to areas mapped as forest by the MODIS

201 land cover map (Friedl et al., 2010) and then further masking these data sets to include only areas

202 where stand age was at least 100 years. The map of stand age reflected conditions c. 2006 and

203 was produced by Pan et al. (2011) by combining forest inventory measurements, information on

204 historical fires, and optical satellite imagery. We applied these 1-km resolution masks to the 250-

205 m resolution BIO_{sat} assuming homogenous land cover and stand age within each 1-km pixel. We

206 then aggregated BIO_{sat} from 250-m to 1-km resolution and computed CRT_{sat} as the ratio of

207 BIO_{sat} to NPP_{sat}.

208

209 **2.1.3 Climate data sets and derivation of the climate moisture index**

210 We quantified water availability using a climate moisture index (CMI) that was computed at

211 monthly time steps as precipitation minus ET_0 (Webb et al., 1983; Hogg, 1994). We summed

212 monthly CMI over each water-year (October in year *t-1* to September in year *t*) from 1985 to

213 2014 and then averaged over years to produce a 30-year climatology ($CMI_{\overline{wy}}$; cm yr^{-1}). The

214 water year represents the approximate annual cycle of soil water recharge and withdrawal

215 (Thomas et al., 2009). We obtained estimates of monthly precipitation from the Parameter-

216 elevation Relationships on Independent Slopes Model (PRISM; Daly et al., 2008), which

217 interpolated weather station measurements onto a 4-km resolution grid. We then estimated

218 monthly ET_0 using the Food and Agricultural Organizations (FAO) Penman-Monteith equation

219 (FAO-56; Allen et al., 1998), where

220
$$ET_0 = \frac{0.408\Delta\,(R_n - G) + \gamma\left(\frac{900}{T + 273}\right)U(e_s - e_a)}{\Delta + \gamma\,(1 + 0.34\,U)}$$

221 Variables included net incoming radiation (R_n), soil heat flux (G), mean daily temperature (T),

222 wind speed (U), and both saturation (e_s) and actual vapor pressure (e_a), as well as the

223 psychrometric constant (γ) and the slope of the vapor pressure curve (Δ). We quantified R_n and U

224 using monthly climatologies from the North American Land Data Assimilation System-2

225 (NALDAS-2; ~12-km resolution) that were based on measurements from 1980-2009 (Mitchell et

226 al., 2004). We derived G, T, e_s, and e_a from PRISM temperature data following Zotarelli et al.

227 (2010). We also computed $CMI_{\overline{wy}}$ based on ET_0 derived using the modified-Hargreaves

228 approach (Hargreaves and Samani, 1985; Droogers and Allen, 2002) and found that our analysis

229 was robust to differences in methods used to compute ET_0 (results not shown). After computing

230 $CMI_{\overline{wy}}$, we then resampled these data using the nearest neighbor approach to match the

231 footprints of both the 1-km NPP and 250-m BIO remote sensing data sets.

232

2.2   Analysis

234 We quantified the response of forest NPP, BIO, and CRT to changes in $CMI_{\overline{wy}}$ across both

235 WAORCA and the broader western US. We specifically focused on areas where $CMI_{\overline{wy}}$ was

236 between -200 and 200 cm yr^{-1}, conditions which occurred both in WAORCA and in the broader

237 region. This range encompassed 98% of forest area in the western US; the paucity of data in the

238 remaining 2% of forest area that was either drier or wetter precluded rigorous analysis. We

239 divided the landscape along this gradient into 10 cm yr^{-1} non-overlapping bins and then

240 summarized forest characteristics in each bin by computing the median, along with the 10th, 25th,

241 75th and 90th percentiles. Forest characteristics were summarized separately for the field and

242 remote sensing data sets. There were a minimum of 10 and a maximum of 114 field sites in each

243 bin. We then assessed the association between the median forest characteristic (i.e., NPP, BIO,

244 and CRT) in each bin and $CMI_{\overline{wy}}$ across the bioclimatic gradient using nonparametric

245 Spearman's rank correlation. This test yields a coefficient (r_s) between -1 and +1, where a value

246 of +1 indicates a perfect monotonically increasing relationship, a value of zero indicates no

247 covariation between the two variables, and a value of -1 indicates a perfect monotonically

248 decreasing relationship. The test is analogous to Pearson's correlation where the data have first

249 been ranked. We assessed the association between forest characteristics and $CMI_{\overline{wy}}$ using

250 Spearman's correlation rather than nonlinear regression because our intent was to describe the

251 general relationship rather than develop a predictive model. We performed data preprocessing,

252   analysis, and visualization using ArcGIS 10 (ESRI, Redlands, CA) and *R* statistical software (R

253   Core Team, 2015), relying extensively on the *R* packages *raster* (Hijmans and van Etten, 2013)

254   and *dplyr* (Wickham and Francois, 2015).

255

256   **3**   **Results**

257   Average annual water availability varied widely across both WAORCA and the broader western

258   US from 1985-2014 (Fig. 1a, b). The $CMI_{\overline{wy}}$ ranged from a minimum of -330 cm yr^{-1} in southern

259   California and Arizona to a maximum of 490 cm yr^{-1} in the Olympic Mountains in northwestern

260   Washington. Forests mapped by MODIS occurred in areas where $CMI_{\overline{wy}}$ was between -340 and

261   490 cm yr^{-1}, though 98% of forest area occurred between -200 and 200 cm y^{-1}, and 72% occurred

262   between -100 and 100 cm yr^{-1}. Average (±1 SD) $CMI_{\overline{wy}}$ in forested areas was -40±80 cm yr^{-1}.

263   The Coast Range and Cascade Mountains in Washington and Oregon were the wettest areas,

264   with $CMI_{\overline{wy}}$ generally >100 cm yr^{-1}. Water availability decreased rapidly in the rain shadows east

265   of the Cascades and Sierra Nevada, giving rise to very steep $CMI_{\overline{wy}}$ gradients. For instance,

266   annual $CMI_{\overline{wy}}$ in northern Oregon decreased nearly 350 cm over ~30 km between high-elevation

267   forests in the Cascades and low-elevation woodlands in the eastern foothills of the Cascades. The

268   range in $CMI_{\overline{wy}}$ encountered along this gradient in the Cascades almost spanned the full range in

269     $CMI_{\overline{wy}}$ that supported 98% of forest area in the western US. Dry forests occurred along the low-

270   elevation margins of mountain ranges throughout continental areas, though the largest tract of

271   dry forest was found in Arizona and New Mexico.

272   Forest NPP, BIO, and BIO residence time varied substantially across both WAORCA and

273 the broader western US in response to variation in $CMI_{\overline{wy}}$ (Fig. 1, 2, Table 2). We focused on

274 forests in areas where $CMI_{\overline{wy}}$ was between -200 and 200 cm yr^{-1} given the paucity of land and

275 measurements in the 2% of forest area that was either drier or wetter. Median $NPP_{field,}$ BIO_{field},

276 and CRT_{field} all exhibited a strong, positive association with $CMI_{\overline{wy}}$ (r_s=0.93-0.96, p<0.001).

277 Median NPP_{field} increased 155% between the driest and wettest 5% of sites in WAORCA (Fig.

278 2a), while median BIO_{field} and CRT_{field} increased 997% and 358%, respectively, between these

279 sites (Fig. 2b, c; Table 2). The relationship in each case was slightly curvilinear. There were also

280 strong, positive relationships among median NPP_{field}, BIO_{field}, and CRT_{field} along the WAORCA

281 bioclimatic gradient (r_s=0.90-0.96, p<0.001).

282   Broadly similar patterns were evident when forest NPP_{sat}, BIO_{sat}, and CRT_{sat} were

283 examined across the western US using remote sensing data sets (Fig. 1b, c, d, 2c, d; Table 2).

284 Median NPP_{sat}, BIO_{sat}, and CRT_{sat} all showed a strong, positive relationship with $CMI_{\overline{wy}}$

285 (r_s=0.93-0.99; p<0.001). Median NPP_{sat} increased 97% between the driest and wettest 5% of

286 forested areas along the regional $CMI_{\overline{wy}}$ gradient (Fig. 2d, Table 2). Similarly, median BIO_{sat} and

287 CRT_{sat} increased 410% and 160%, respectively, between the driest and wettest areas (Fig. 2e, f,

288 Table 2). The response of median NPP_{sat}, BIO_{sat}, and CRT_{sat} to increased $CMI_{\overline{wy}}$ was more

289 curvilinear than the field measurements and plateaued in areas where $CMI_{\overline{wy}}$ exceeded ~100 cm

290 yr^{-1}. Furthermore, while magnitude of NPP_{sat} and NPP_{field} response to $CMI_{\overline{wy}}$ were similar, the

291 magnitude of BIO_{sat} and CRT_{sat} responses to increased $CMI_{\overline{wy}}$ were much more muted than the

292 magnitude of response in BIO_{field} and CRT_{field}. Nevertheless, field- and satellite-derived

293 estimates of median NPP, BIO, and CRT were strongly correlated (r_s=0.90-0.95; p<0.001).

294 Furthermore, there were again strong relationships among median NPP_{sat}, BIO_{sat}, and CRT_{sat}

295 along the western US bioclimatic gradient (r_s=0.93-0.97, p<0.001).

296

297 **4   Discussion and conclusions**

298 **4.1   Climate moisture index**

299 Water availability exerted a strong influence on NPP, BIO, and CRT among mature forests in the

300 western US. We chose to quantify water availability using an index that accounted for both

301 precipitation and energy-mediated ET_0, recognizing that both of these factors contribute to the

302 relative water stress experienced by plants within an ecosystem (Webb et al., 1983). We

303 acknowledge that this index has several short-comings. For instance, the index does not account

304 for spatial variation in soil water storage capacity, which can be crucial for determining plant

305 performance during drought (Peterman et al., 2013). This might explain some of the variation in

306 NPP and BIO among areas with similar $CMI_{\overline{wy}}$; however, quantifying soil water storage capacity

307 even at individual sites is challenging given uncertainty in soil structure and plant rooting

308 capacity (Running, 1994). The index also does not account for water added via fog drip, which

309 has been shown to supply 13-45% of the water transpired by redwood forests (*S. sempervirens*)

310 (Dawson, 1998) and sustain other forest ecosystems along the California coast (Johnstone and

311 Dawson, 2010; Fischer et al., 2016). This potentially explains why there were areas with low

312 $CMI_{\overline{wy}}$ along the central and northern coast of California that supported forests with higher NPP

313 and BIO than other forests with similar $CMI_{\overline{wy}}$. Furthermore, the index does not account for

314 spatial variation in runoff and thus likely overestimates water availability in the wettest areas

315   since the fraction of water lost as run-off increases with precipitation (Sanford and Selnick,

316   2013). Despite its relative simplicity, prior studies showed that CMI was a useful index for

317   explaining interannual variability in fire activity in the southwest US (Williams et al., 2014), as

318   well as forest productivity in northern Siberia (Berner et al., 2013), southern Canada (Hogg et al.,

319   2002), and central Oregon (Berner and Law, 2015). Several studies also found that the index, or

320   its inverse (i.e. ET_0 - P), explained substantial spatial variability in mature forest gross

321   photosynthesis (Law et al., 2002), productivity and biomass across a range of ecosystems (Webb

322   et al., 1983; Hogg et al., 2008; Berner and Law, 2015). Our current study further demonstrates

323   that CMI is a useful, empirical index for assessing climatic constraints on forest ecosystems at

324   large spatial scales.

325

4.2   Tree net primary productivity

327   Median forest NPP in mature stands approximately doubled between the driest and wettest areas

328   in both WAORCA and the western US, though in both cases the rate at which NPP increased

329   with $CMI_{\overline{wy}}$ slowed in the wettest areas. Prior field studies conducted at a limited number of field

330   sites in the western US over the past four decades have similarly documented increased forest

331   NPP along spatial gradients of increasing water availability (Whittaker and Niering, 1975;

332   Gholz, 1982; Webb et al., 1983; Berner and Law, 2015). Building on these prior efforts, our

333   current study demonstrates a robust relationship between mature forest NPP and water

334   availability using field measurements from nearly 2,000 inventory plots along with satellite

335   remote sensing estimates of NPP covering ~18 Mha of forestland.

336  The NPP-CMI$_{\overline{wy}}$ relationship was similar when NPP was assessed using field

337 measurements from across WAORCA or using MODIS covering the western US. MODIS did

338 show NPP leveling off in the wettest parts of WAORCA (CMI$_{\overline{wy}} \approx$ 100-200 cm yr^{-1}), whereas

339 this was less evident in the field measurements. The inventory sites and MODIS forestland

340 occurred at similar elevations along the CMI$_{\overline{wy}}$ gradient in WAORCA, suggesting that this

341 discrepancy in NPP was not due to MODIS systematically including cold, high-elevation areas

342 not sampled by the inventory sites. One possibility is that MODIS NPP did not increase in the

343 wettest areas because MODIS becomes less sensitive to increases in the fraction of

344 photosynthetically-active radiation (FPAR) absorbed by plant canopies in densely vegetated

345 areas (Yan et al., 2016). A recent MODIS analysis similarly found that the amount of

346 photosynthetically-active radiation absorbed by plant canopies (APAR = FPAR x PAR)

347 increased asymptotically with increasing mean annual precipitation across plant communities in

348 California (Jin and Goulden, 2014). Forests had higher APAR than other plant communities and,

349 furthermore, exhibited the smallest increase in APAR per unit increase in precipitation of any

350 plant community, suggesting that forest productivity was less sensitive to changes in

351 precipitation than productivity of other plant communities (Jin and Goulden, 2014). In contrast

352 with the field measurements, the asymptotic response of MODIS NPP and APAR to increasing

353 water availability in wet areas suggests that climate impact assessments based on MODIS could

354 underestimate the sensitivity of plant productivity to changes in water availability in wet areas

355 with high biomass.

356  Mechanistically, the strong NPP-CMI$_{\overline{wy}}$ association reflects the coupling between carbon

357 and water cycling at leaf (Ball et al., 1987) to ecosystem scales (Law et al., 2002). Forest NPP

358 depends on regionally-specific relations with leaf area (Schroeder et al., 1982; Waring, 1983),

359 which largely determine the proportion of incoming solar radiation that is absorbed and thus

360 potentially available to fuel photosynthesis (Runyon et al., 1994). Leaf photosynthesis inevitably

361 leads to transpiration water loss (Ball et al., 1987) that must be balanced against water uptake

362 from the soil so as to prevent the formation of excessive tension on the internal water column

363 that could result in hydraulic failure (Williams et al., 1996; Ruehr et al., 2014). As soil water

364 availability increases, trees are able to support greater leaf area while maintaining water column

365 tensions within physiologically operable ranges, which consequently leads to more

366 photosynthate available to fuel NPP unless trees are limited by other resources (e.g., nitrogen).

367 The decreasing rate at which NPP increased with $CMI_{\overline{wy}}$ in the wettest areas is likely due to low

368 temperatures constraining productivity at high-elevations (Runyon et al., 1994; Nakawatase and

369 Peterson, 2006) and heavy cloud-cover limiting solar radiation and thus photosynthesis in coastal

370 areas (Zhao et al., 2010; Carroll et al., 2014). Forest NPP is affected by many biotic (e.g., age)

371 and abiotic factors (e.g., nutrients), yet water availability emerges as a key environmental

372 constraint in the western US.

373

374 **4.3   Tree carbon stocks**

375 Mature forest BIO increased notably with increasing $CMI_{\overline{wy}}$ across both WAORCA and the

376 broader western US, reflecting underlying shifts in NPP and, likely, BIO mortality rates due to

377 natural disturbance. BIO is determined by the rates at which carbon is gained via NPP and lost

378 due to tissue senescence and mortality integrated over annual to centennial time scales (Olson,

379 1963). Hence, the increase in NPP with increasing $CMI_{\overline{wy}}$ explains some of the concomitant

380 increase in BIO. Our analysis did not investigate how tissue senescence or mortality varied along

381 the regional bioclimatic gradient, though a recent study found that BIO mortality rates due to

382 bark beetles and fires were very low in the wettest parts of the western US (e.g., Coast Range

383 and Cascades), while considerably higher in most drier areas (Hicke et al., 2013). Furthermore,

384 the field and satellite data sets also incidentally revealed there was an increase in the median age

385 of stands over 100 years as conditions became wetter, with median stand age ~140 years in the

386 driest areas and 200-240 years in the wettest areas. The general increase in mature forest BIO

387 with increasing water availability is thus likely due to higher rates of productivity and potentially

388 lower BIO mortality rates from natural disturbance.

389   The observed increase in mature forest BIO with increasing water availability was

390 generally consistent with prior field studies from this region, yet our study demonstrates this

391 response over a much broader bioclimatic gradient. For instance, early work by Whittaker and

392 Niering (1975) showed that mature forest BIO tended to increase with a moisture index inferred

393 from community composition along an elevational gradient in Arizona's Santa Catalina

394 Mountains. Subsequent studies focused on five LTER sites spread across the conterminous US

395 (Webb et al., 1983) and at 8-12 sites in Oregon (Gholz, 1982; Berner and Law, 2015) similarly

396 showed a general increase in tree biomass with increasing water availability. Our study included

397 sites that ranged from dry woodlands with little BIO to temperate rainforests with BIO exceeded

398 in few other regions (e.g. max BIO $\approx$ 950 Mg C ha^{-1}). BIO in our study area has been reported to

399 reach over 2,000 Mg C ha^{-1} in old-growth coastal redwood stands in northern California (Waring

400 and Franklin, 1979), which is thought to be exceeded only by the >3,000 Mg C ha^{-1} attained by

401 old-growth *Eucalyptus regnans* stands in southern Australia (Keith et al., 2009). A global

402 synthesis suggested that average AGB among high-biomass stands in wet temperate forests

403 (~377 Mg C ha^{-1}) was over twice that of high-biomass stands in wet tropical forests (~179 Mg C

404   ha^{-1}) and nearly six times that of high-biomass stands in wet boreal forests (~64 Mg C ha^{-1})

405   (Keith et al., 2009). The range in mature forest BIO included in our analysis of WAORCA thus

406   spanned much of the observed global range in BIO.

407   Both field and satellite measurements revealed that median BIO increased with $CMI_{\overline{wy}}$,

408   yet the satellite data set showed less of an increase than the field measurements. Median forest

409   BIO_{field} increased nearly 1,000% between the dry woodlands and coastal temperate rainforests in

410   WAORCA, yet the increase in BIO_{sat} with increasing $CMI_{\overline{wy}}$ was less pronounced (~410%

411   increase) when assessed across the western US. Furthermore, median BIO_{sat} plateaued around

412   175 Mg C ha^{-1} in areas where $CMI_{\overline{wy}}$ was ~100-200 cm yr^{-1}. The response of BIO to increasing

413    $CMI_{\overline{wy}}$ was likely more muted when assessed using the satellite-derived maps than the field

414   measurements for several reasons. The maps are largely derived from optical, multi-spectral

415   satellite imagery that is not very sensitive to variation in BIO in high-biomass forests.

416   Additionally, areas with high BIO often occur as small patches set in a matrix of stands with

417   lower BIO (Spies et al., 1994) and thus the moderate-resolution satellite imagery used in

418   developing these maps records the spectral signature of this larger area rather than just the patch

419   with high BIO. In other words, the satellite imagery has a larger sampling footprint relative to

420   that of a field plot, which thus averages BIO over a larger area, reducing peak values. Advances

421   in satellite remote sensing, such as NASA's new Global Ecosystem Dynamics Investigation

422   Lidar (GEDI) instrument, are anticipated to help overcome some of these challenges (Goetz and

423   Dubayah, 2011). Nevertheless, current BIO maps (e.g., Kellndorfer et al., 2012; Wilson et al.,

424   2013) proved a valuable tool for ecologic and natural resource assessments (Berner et al., 2012;

425   Goetz et al., 2014; Krankina et al., 2014).

426

4.4 Carbon residence time in tree biomass

428 We computed CRT as BIO/NPP and found that median CRT_{field} increased persistently with

429 $CMI_{\overline{wy}}$ from ~11 years in the driest forests to over 49 years in the wettest forests, highlighting a

430 fundamental change in ecosystem function along this broad bioclimatic gradient. One limitation

431 of our study is that computing CRT in this manner assumes that BIO is constant over time

432 (Friend et al., 2014). We focused on mature stands (>100 years) to minimize the change in BIO

433 over time, though acknowledge that BIO can gradually increase during subsequent centuries

434 (Hudiburg et al., 2009), which would lead us to underestimated CRT. Conversely, drought and

435 insect-induced defoliation in the early 2000s could have suppressed NPP (Schwalm et al., 2012;

436 Berner and Law, 2015) without a proportional reduction in BIO, which could have inflated our

437 estimates of CRT in some areas. Nevertheless, our results agree well with a prior study focused

438 on 11 LTERS spread across the conterminous US that found CRT increased from ~2 years in a

439 desert shrubland to ~73 years in 450-years old Douglas-fir stand at the Andrews LTER in the

440 Oregon Cascade Mountains (Webb et al., 1983). For comparison, we looked at five old-growth

441 Douglas-fir stands (336-555 years old) near the Andrews LTER and found that CRT_{field} averaged

442 79±23 years (± 1SD) among these stands. An increase in the CRT of aboveground tissues was

443 also observed among plant communities along an elevational moisture gradient in the Santa

444 Catalina Mountains of Arizona (Whittaker and Niering, 1975) and across nine mature stands in a

445 range of forest communities in Oregon (Gholz, 1982). Although this pattern has been previously

446 documented at small scales, the underlying mechanisms remain unclear.

447   We speculate that the increase in CRT with increased water availability was associated

448   with underlying changes in NPP allocation, BIO mortality rates, and stand age. Trees invest a

449   larger proportion of NPP into aboveground tissue production as conditions become wetter and

450   competition for light intensifies (Runyon et al., 1994; Law et al., 2003). Our field measurements

451   revealed that the fraction of NPP allocated aboveground increased from ~0.45 in the driest areas

452   to ~0.64 in the wettest areas and, furthermore, that CRT in aboveground tissues averaged twice

453   as long as CRT in belowground tissues. Thus, a shift in NPP allocation toward longer-lived

454   aboveground tissues likely contributed to longer CRT in wetter areas. Longer CRT in wetter

455   areas could also be related to forests in these areas (e.g., Coast Range) experiencing lower BIO

456   mortality rates from wildfire and bark beetles than forests in drier, continental areas (Hicke et al.,

457   2013). We also found that mature stands tended to be older in wetter areas and that older stands

458   tended to have longer CRT, likely as a result of these stands having higher BIO and similar NPP

459   (Hudiburg et al., 2009). Consequently, the CRT-$CMI_{\overline{wy}}$ relationships that we observed

460   incorporate an age-related effect; however, the effect was quite small relative to the climate-

461   effect. This can be illustrated by comparing median CRT between mature (100-200 years) and

462   old (>200 years) stands occupying very dry ($CMI_{\overline{wy}} < -100$ cm yr^{-1}) and very wet ($CMI_{\overline{wy}} > 100$

463   cm yr^{-1}) areas. Median CRT differed by 6% (16 vs. 17 years) between mature and old stands in

464   very dry areas and by 10% (47 vs. 52 years) in very wet areas. Conversely, median CRT of

465   mature stands differed 98% (16 vs. 47 years) between very dry and very wet areas, while the

466   median CRT of old stands differed 101% (52 vs. 17 years) between very dry and very wet areas.

467   In other words, the difference in CRT between stands in contrasting climates is much greater

468   than difference in CRT between mature and old stands within a climate zone. Our study

469   demonstrates that CRT in live tree biomass was strongly influenced by water availability, yet

470   additional efforts are needed to determine the underlying mechanism by which changes in water

471   availability affect CRT, particularly given that CRT is a primary source of uncertainty in global

472   vegetation model projections of future terrestrial carbon cycling (Friend et al., 2014).

473

4.5   Predicting ecosystem response to environmental change

475   Water availability is projected to decline in much of the western US over the coming century, in

476   part due to higher temperatures increasing atmospheric evaporative demand (Dai, 2013; Walsh et

477   al., 2014; Cook et al., 2015). Predicting the timing, magnitude and extent of ecological response

478   to regional climate change remains a challenge. Our study showed that water availability is a key

479   determinant of forest structure and function in the western US, broadly suggesting that chronic

480   reductions in regional water availability could reduce the NPP, BIO, and CRT of mature stands.

481   Nevertheless, it is problematic to predict the temporal response of extant forest communities to

482   near-term climatic change based on bioclimatic relationships derived from spatial data. For

483   instance, recent studies found that the slope of the NPP-precipitation relationship was much

484   steeper when derived from spatial data than when derived from the temporal response of NPP to

485   interannual variation in precipitation (Jin and Goulden, 2014; Wilcox et al., 2016). Near-term

486   effects of climate variability depend on the physiological characteristics of species in the extant

487   plant community, yet bioclimatic relationships derived from spatial data reflect gradual

488   adjustment of community composition and population size to climate over long periods of time

489   (Jin and Goulden, 2014; Wilcox et al., 2016). Furthermore, bioclimatic models derived from

490   spatial data cannot account for other ecophysiological impacts of environmental change, such as

491   (1) enhanced plant water use efficiency from CO_2 fertilization (Soulé and Knapp, 2015); (2)

492   increased likelihood of tree mortality due to hotter drought (Adams et al., 2009); or (3) novel

493   changes in disturbance regimes (Dale et al., 2001; Hicke et al., 2006). Consequently, predicting

494   ecological response to environmental change over the coming century will require the use of

495   mechanistic ecosystem models that account for physiologic, demographic, and disturbance

496   processes at fine taxonomic and spatial scales (Hudiburg et al., 2013; Law, 2014). Although

497   spatial models may not be suitable for near-term projection of ecosystems change, they do

498   provide insight into long-term ecosystem adaptation to local climate and, furthermore, can be

499   used to validate and refine mechanistic models if constructed from a representative sample of

500   forestlands.

501

502   **4.6   Summary and conclusions**

503   Water availability varies widely across the western US, giving rise to forests that range from dry,

504   low-biomass woodlands to temperate rainforests that are among highest biomass forests found

505   anywhere in the world. In this study we quantified changes in tree productivity, live biomass, and

506   carbon residence time along spatial gradients in water availability using field inventory

507   measurements from WAORCA and satellite remote sensing data sets spanning the western US.

508   Our multi-method, multi-scale analysis revealed that tree productivity, live biomass, and carbon

509   residence time all increased notably with water availability, which we computed using an index

510   that accounted for both precipitation and reference evapotranspiration. The observed increase in

511   productivity was likely due to the close coupling between carbon and water cycling at leaf to

512   ecosystem scales, while the observed increase in live biomass was associated with higher

513   productivity and longer carbon residence. The increase in carbon residence time in wetter areas

514 was linked with greater carbon allocation to long-lived aboveground tissues, older stand age,

515 and, possibly, lower biomass mortality rates from natural disturbance (e.g., bark beetles, fires).

516 Tree productivity and biomass derived from field- and satellite-measurements exhibited similar

517 responses to increasing water availability, though the satellite data sets tended to plateau in the

518 wettest areas, suggesting that additional efforts are needed to better quantify productivity and

519 biomass from satellites in high-productivity, high-biomass forests. The pronounced increase in

520 tree productivity, biomass, and carbon residence time between the driest and wettest areas

521 illustrates the gradual adjustment of ecosystem structure and function to long-term variation in

522 water availability; however, the observed bioclimatic relationships are not suitable for near-term

523 projections of future ecosystem response to regional drying. Predicting near-term ecosystem

524 response to drying and other environmental change (e.g., increased CO_2) will require

525 mechanistic ecosystem models, which can be evaluated against bioclimatic relationships

526 developed using inventory sites from a representative sample of forestlands (e.g., Forest Service

527 inventory sites). Overall, our results indicate that water availability is a key determinant of tree

528 productivity, live biomass, and carbon residence time in mature stands ranging from dry

529 woodlands to coastal temperate rainforests. Future efforts are needed to anticipate and mitigate

530 the impacts of projected warming and drying on forest ecosystems in the western US and

531 elsewhere around the world.

532

533 **Author contributions**

534 L.T.B. designed the study, analyzed the data, and prepared the manuscript with contributions

535 from B.E.L. and T.W.H., who both also contributed data sets to this effort.

536

Acknowledgements

538 This work was supported by NASA Headquarters under the NASA Earth and Space Science

539 Fellowship Program (Grant NNX14AN65H), the USDA National Institute of Food and

540 Agriculture (Grant 2013-67003-20652), and the ARCS Foundation Scholar program. T.W.H.

541 was supported by the National Science Foundation Idaho EPSCoR Program (Grant IIA-

542 1301792). We thank the researchers who provided the geospatial data sets used in this analysis.

543 We cite no conflicts of interest.

544

References

546 Adams, H. D., Guardiola-Claramonte, M., Barron-Gafford, G. A., Villegas, J. C., Breshears, D. D., Zou, C. B.,
547 Troch, P. A., and Huxman, T. E.: Temperature sensitivity of drought-induced tree mortality portends
548 increased regional die-off under global-change-type drought, Proceedings of the National Academy of
549 Sciences of the United States of America, 106, 7063-7066, 10.1073/pnas.0901438106, 2009.
550 Allen, R. G., Pereira, L. S., Raes, D., and Smith, M.: Crop evapotranspiration-Guidelines for computing
551 crop water requirements-FAO Irrigation and drainage paper 56, FAO, Rome, 300, 1998.
552 Ball, J. T., Woodrow, I. E., and Berry, J. A.: A model predicting stomatal conductance and its contribution
553 to the control of photosynthesis under different environmental conditions, in: Progress in
554 photosynthesis research, Springer, 221-224, 1987.
555 Bechtold, W., and Patterson, P.: The enhanced forest inventory and analysis program-- national
556 sampling design and estimation procedures, USDA Forest Service General Technical Report SRS-80,
557 Asheville, NC, 98, 2005.
558 Berner, L. T., Beck, P. S. A., Loranty, M. M., Alexander, H. D., Mack, M. C., and Goetz, S. J.: Cajander larch
559 (Larix cajanderi) biomass distribution, fire regime and post-fire recovery in northeastern Siberia,
560 Biogeosciences, 9, 3943-3959, 10.5194/bg-9-3943-2012, 2012.
561 Berner, L. T., Beck, P. S. A., Bunn, A. G., and Goetz, S. J.: Plant response to climate change along the
562 forest-tundra ecotone in northeastern Siberia, Global Change Biology, 19, 3449-3462,
563 10.1111/gcb.12304, 2013.
564 Berner, L. T., and Law, B. E.: Water limitations on forest carbon cycling and conifer traits along a steep
565 climatic gradient in the Cascade Mountains, Oregon, Biogeosciences, 12, 6617-6635, 2015.
566 Berner, L. T., and Law, B. E.: Plant traits, productivity, biomass and soil properties from forest sites in the
567 Pacific Northwest, 1999–2014, Scientific Data, 3, 160002, 10.1038/sdata.2016.2, 2016.

568 Blackard, J., Finco, M., Helmer, E., Holden, G., Hoppus, M., Jacobs, D., Lister, A., Moisen, G., Nelson, M.,
569 and Riemann, R.: Mapping US forest biomass using nationwide forest inventory data and moderate
570 resolution information, Remote Sensing of Environment, 112, 1658-1677, 2008.
571 Cairns, M. A., Brown, S., Helmer, E. H., and Baumgardner, G. A.: Root biomass allocation in the world's
572 upland forests, Oecologia, 111, 1-11, 1997.
573 Carroll, A. L., Sillett, S. C., and Kramer, R. D.: Millennium-Scale Crossdating and Inter-Annual Climate
574 Sensitivities of Standing California Redwoods, PLoS ONE, 9, e102545, 10.1371/journal.pone.0102545,
575 2014.
576 Churkina, G., and Running, S. W.: Contrasting climatic controls on the estimated productivity of global
577 terrestrial biomes, Ecosystems, 1, 206-215, 1998.
578 Collins, M., Knutti, R., Arblaster, J., Dufresne, J.-L., Fichefet, T., Friedlingstein, P., Gao, X., Gutowski, W. J.,
579 Johns, T., Krinner, G., Shongwe, M., Tebaldi, C., Weaver, A. J., and Wehner, M.: Long-term Climate
580 Change: Projections, Commitments and Irreversibility, in: Climate Change 2013: The Physical Science
581 Basis. Contribution of Working Group I to the Fifth Assessment Report of the Intergovernmental Panel
582 on Climate Change, edited by: Stocker, T. F., Qin, D., Plattner, G.-K., Tignor, M., Allen, S. K., Boschung, J.,
583 Nauels, A., Xia, Y., Bex, V., and Midgley, P. M., Cambridge University Press, Cambridge, United Kingdom
584 and New York, NY, USA, 1029–1136, 2013.
585 Cook, B. I., Ault, T. R., and Smerdon, J. E.: Unprecedented 21st century drought risk in the American
586 Southwest and Central Plains, Science Advances, 1, e1400082, 2015.
587 Dai, A.: Increasing drought under global warming in observations and models, Nature Climate Change, 3,
588 52-58, doi: 10.1038/nclimate1633, 2013.
589 Dale, V. H., Joyce, L. A., McNulty, S., Neilson, R. P., Ayres, M. P., Flannigan, M. D., Hanson, P. J., Irland, L.
590 C., Lugo, A. E., Peterson, C. J., Simberloff, D., Swanson, F. J., Stocks, B. J., and Michael Wotton, B.:
591 Climate Change and Forest Disturbances, BioScience, 51, 723-734, 10.1641/0006-
592 3568(2001)051[0723:ccafd]2.0.co;2, 2001.
593 Daly, C., Halbleib, M., Smith, J. I., Gibson, W. P., Doggett, M. K., Taylor, G. H., Curtis, J., and Pasteris, P. P.:
594 Physiographically sensitive mapping of climatological temperature and precipitation across the
595 conterminous United States, International Journal of Climatology, 28, 2031-2064, 2008.
596 Dawson, T. E.: Fog in the California redwood forest: ecosystem inputs and use by plants, Oecologia, 117,
597 476-485, 1998.
598 Droogers, P., and Allen, R. G.: Estimating reference evapotranspiration under inaccurate data conditions,
599 Irrigation and drainage systems, 16, 33-45, 2002.
600 Fischer, D. T., Still, C. J., Ebert, C. M., Baguskas, S. A., and Park Williams, A.: Fog drip maintains dry
601 season ecological function in a California coastal pine forest, Ecosphere, 7, 2016.
602 Friedl, M. A., Sulla-Menashe, D., Tan, B., Schneider, A., Ramankutty, N., Sibley, A., and Huang, X.: MODIS
603 Collection 5 global land cover: Algorithm refinements and characterization of new datasets, Remote
604 Sensing of Environment, 114, 168-182, 2010.
605 Friend, A. D., Lucht, W., Rademacher, T. T., Keribin, R., Betts, R., Cadule, P., Ciais, P., Clark, D. B.,
606 Dankers, R., and Falloon, P. D.: Carbon residence time dominates uncertainty in terrestrial vegetation
607 responses to future climate and atmospheric CO2, Proceedings of the National Academy of Sciences,
608 111, 3280-3285, 2014.
609 Gholz, H. L.: Environmental Limits on Aboveground Net Primary Production, Leaf Area, and Biomass in
610 Vegetation Zones of the Pacific Northwest, Ecology, 63, 469-481, 10.2307/1938964, 1982.
611 Girardin, C. A. J., Malhi, Y., Aragao, L., Mamani, M., Huaraca Huasco, W., Durand, L., Feeley, K., Rapp, J.,
612 SILVA-ESPEJO, J., and Silman, M.: Net primary productivity allocation and cycling of carbon along a
613 tropical forest elevational transect in the Peruvian Andes, Global Change Biology, 16, 3176-3192, 2010.

614   Goetz, S., and Dubayah, R.: Advances in remote sensing technology and implications for measuring and
615   monitoring forest carbon stocks and change, Carbon Management, 2, 231-244, 10.4155/cmt.11.18,
616   2011.
617   Goetz, S. J., Sun, M., Zolkos, S., Hansen, A., and Dubayah, R.: The relative importance of climate and
618   vegetation properties on patterns of North American breeding bird species richness, Environmental
619   Research Letters, 9, 034013, 2014.
620   Hargreaves, G. H., and Samani, Z. A.: Reference crop evapotranspiration from temperature, Applied
621   Engineering in Agriculture, 1, 96-99, 1985.
622   Hicke, J. A., Logan, J. A., Powell, J., and Ojima, D. S.: Changing temperatures influence suitability for
623   modeled mountain pine beetle (Dendroctonus ponderosae) outbreaks in the western United States,
624   Journal of Geophysical Research: Biogeosciences (2005–2012), 111, 2006.
625   Hicke, J. A., Meddens, A. J., Allen, C. D., and Kolden, C. A.: Carbon stocks of trees killed by bark beetles
626   and wildfire in the western United States, Environmental Research Letters, 8, 035032, 2013.
627   Hijmans, R. J., and van Etten, J.: raster: Geographic analysis and modeling with raster data, 2.1-25 ed., R
628   Foundation for Statistical Computing, Vienna, 2013.
629   Hogg, E., Brandt, J. P., and Kochtubajda, B.: Growth and dieback of aspen forests in northwestern
630   Alberta, Canada, in relation to climate and insects, Canadian Journal of Forest Research, 32, 823-832,
631   2002.
632   Hogg, E., Brandt, J., and Michaelian, M.: Impacts of a regional drought on the productivity, dieback, and
633   biomass of western Canadian aspen forests, Canadian Journal of Forest Research, 38, 1373-1384, 2008.
634   Hogg, E. H.: Climate and the southern limit of the western Canadian boreal forest, Canadian Journal of
635   Forest Research, 24, 1835-1845, 1994.
636   Hogg, E. H., and Hurdle, P.: The aspen parkland in western Canada: A dry-climate analogue for the future
637   boreal forest?, Water, Air, and Soil Pollution, 82, 391-400, 1995.
638   Holdridge, L. R.: Determination of World Plant Formations From Simple Climatic Data, Science, 105, 367-
639   368, 10.1126/science.105.2727.367, 1947.
640   Hudiburg, T., Law, B., Turner, D. P., Campbell, J., Donato, D., and Duane, M.: Carbon dynamics of Oregon
641   and Northern California forests and potential land-based carbon storage, Ecological Applications, 19,
642   163-180, 2009.
643   Hudiburg, T. W., Law, B. E., Wirth, C., and Luyssaert, S.: Regional carbon dioxide implications of forest
644   bioenergy production, Nature Climate Change, 1, 419-423, 10.1038/nclimate1264, 2011.
645   Hudiburg, T. W., Law, B. E., and Thornton, P. E.: Evaluation and improvement of the Community Land
646   Model (CLM4) in Oregon forests, Biogeosciences, 10, 453-470, 10.5194/bg-10-453-2013, 2013.
647   Jin, Y., and Goulden, M. L.: Ecological consequences of variation in precipitation: separating short-versus
648   long-term effects using satellite data, Global Ecology and Biogeography, 23, 358-370, 2014.
649   Johnstone, J. A., and Dawson, T. E.: Climatic context and ecological implications of summer fog decline in
650   the coast redwood region, Proceedings of the National Academy of Sciences, 107, 4533-4538, 2010.
651   Keith, H., Mackey, B. G., and Lindenmayer, D. B.: Re-evaluation of forest biomass carbon stocks and
652   lessons from the world's most carbon-dense forests, Proceedings of the National Academy of Sciences,
653   106, 11635-11640, 2009.
654   Kellndorfer, J., Walker, W., LaPoint, E., Bishop, J., Cormier, T., Fiske, G., Hoppus, M., Kirsch, K., and
655   Westfall, J.: NACP Aboveground Biomass and Carbon Baseline Data (NBCD 2000), U.S.A., 2000 Data set,
656   ORNL DAAC, Oak Ridge, Tennessee, U.S.A. , 2012.
657   Krankina, O. N., DellaSala, D. A., Leonard, J., and Yatskov, M.: High-Biomass Forests of the Pacific
658   Northwest: Who Manages Them and How Much is Protected?, Environmental Management, 54, 112-
659   121, 2014.

660 Law, B. E., Thornton, P. E., Irvine, J., Anthoni, P. M., and Van Tuyl, S.: Carbon storage and fluxes in
661 ponderosa pine forests at different developmental stages, Global Change Biology, 7, 755-777, 2001.
662 Law, B. E., Falge, E., Gu, L. V., Baldocchi, D. D., Bakwin, P., Berbigier, P., Davis, K., Dolman, A. J., Falk, M.,
663 and Fuentes, J. D.: Environmental controls over carbon dioxide and water vapor exchange of terrestrial
664 vegetation, Agricultural and Forest Meteorology, 113, 97-120, 2002.
665 Law, B. E., Sun, O. J., Campbell, J., Van Tuyl, S., and Thornton, P. E.: Changes in carbon storage and fluxes
666 in a chronosequence of ponderosa pine, Global Change Biology, 9, 510-524, 2003.
667 Law, B. E.: Regional analysis of drought and heat impacts on forests: current and future science
668 directions, Global Change Biology, 20, 3595-3599, 10.1111/gcb.12651, 2014.
669 Major, J.: A climatic index to vascular plant activity, Ecology, 44, 485-498, 1963.
670 Means, J. E., Hansen, H. A., Koerper, G. J., Alaback, P. B., and Klopsch, M. W.: Software for computing
671 plant biomass--BIOPAK users guide, U.S. Department of Agriculture, Forest Service, Pacific Northwest
672 Research Station, Portland, OR, 184, 1994.
673 Mitchell, K. E., Lohmann, D., Houser, P. R., Wood, E. F., Schaake, J. C., Robock, A., Cosgrove, B. A.,
674 Sheffield, J., Duan, Q., and Luo, L.: The multi-institution North American Land Data Assimilation System
675 (NLDAS): Utilizing multiple GCIP products and partners in a continental distributed hydrological
676 modeling system, Journal of Geophysical Research: Atmospheres, 109, 2004.
677 Myneni, R., Hoffman, S., Knyazikhin, Y., Privette, J., Glassy, J., Tian, Y., Wang, Y., Song, X., Zhang, Y., and
678 Smith, G.: Global products of vegetation leaf area and fraction absorbed PAR from year one of MODIS
679 data, Remote sensing of environment, 83, 214-231, 2002.
680 Nakawatase, J. M., and Peterson, D. L.: Spatial variability in forest growth-climate relationships in the
681 Olympic Mountains, Washington, Canadian journal of forest research, 36, 77-91, 2006.
682 Neeti, N., and Kennedy, R.: Comparison of national level biomass maps for conterminous US:
683 understanding pattern and causes of differences, Carbon Balance and Management, 11, 19,
684 10.1186/s13021-016-0060-y, 2016.
685 Olson, J. S.: Energy storage and the balance of producers and decomposers in ecological systems,
686 Ecology, 44, 322-331, 1963.
687 Pan, Y., Chen, J. M., Birdsey, R., McCullough, K., He, L., and Deng, F.: Age structure and disturbance
688 legacy of North American forests, 2011.
689 Peterman, W., Waring, R. H., Seager, T., and Pollock, W. L.: Soil properties affect pinyon pine–juniper
690 response to drought, Ecohydrology, 6, 455-463, 2013.
691 R Core Team: R: A Language and Environment for Statistical Computing, R Foundation for Statistical
692 Computing, Vienna, 2015.
693 Ruefenacht, B., Finco, M., Nelson, M., Czaplewski, R., Helmer, E., Blackard, J., Holden, G., Lister, A.,
694 Salajanu, D., and Weyermann, D.: Conterminous US and Alaska forest type mapping using forest
695 inventory and analysis data, Photogramm. Eng. Remote Sens, 74, 1379-1388, 2008.
696 Ruehr, N., Law, B., Quandt, D., and Williams, M.: Effects of heat and drought on carbon and water
697 dynamics in a regenerating semi-arid pine forest: a combined experimental and modeling approach,
698 Biogeosciences, 11, 4139-4156, 2014.
699 Running, S. W.: Testing Forest-BGC Ecosystem Process Simulations Across a Climatic Gradient in Oregon,
700 Ecological Applications, 4, 238-247, 1994.
701 Running, S. W., Nemani, R. R., Heinsch, F. A., Zhao, M., Reeves, M., and Hashimoto, H.: A continuous
702 satellite-derived measure of global terrestrial primary production, BioScience, 54, 547-560, 2004.
703 Runyon, J., Waring, R., Goward, S., and Welles, J.: Environmental limits on net primary production and
704 light-use efficiency across the Oregon transect, Ecological Applications, 4, 226-237, 1994.

705   Sanford, W. E., and Selnick, D. L.: Estimation of Evapotranspiration Across the Conterminous United
706   States Using a Regression With Climate and Land-Cover Data1, JAWRA Journal of the American Water
707   Resources Association, 49, 217-230, 2013.
708   Schroeder, P. E., McCandlish, B., Waring, R. H., and Perry, D. A.: The relationship of maximum canopy
709   leaf area to forest growth in eastern Washington, Northwest Science, 56, 121-130, 1982.
710   Schuur, E. A.: Productivity and global climate revisited: the sensitivity of tropical forest growth to
711   precipitation, Ecology, 84, 1165-1170, 2003.
712   Schwalm, C. R., Williams, C. A., Schaefer, K., Baldocchi, D., Black, T. A., Goldstein, A. H., Law, B. E.,
713   Oechel, W. C., and Scott, R. L.: Reduction in carbon uptake during turn of the century drought in western
714   North America, Nature Geoscience, 5, 551-556, 2012.
715   Smith, J. E., Heath, L. S., Skog, K. E., and Birdsey, R. A.: Methods for calculating forest ecosystem and
716   harvested carbon with standard estimates for forest types of the United States, USDA Forest Service
717   General Technical Report NE-343, Newtown Square, PA, 222, 2006.
718   Soulé, P. T., and Knapp, P. A.: Analyses of intrinsic water-use efficiency indicate performance differences
719   of ponderosa pine and Douglas-fir in response to CO_2 enrichment, Journal of Biogeography, 42, 144-
720   155, 2015.
721   Spies, T. A., Ripple, W. J., and Bradshaw, G.: Dynamics and pattern of a managed coniferous forest
722   landscape in Oregon, Ecological Applications, 4, 555-568, 1994.
723   Thomas, C. K., Law, B. E., Irvine, J., Martin, J. G., Pettijohn, J. C., and Davis, K. J.: Seasonal hydrology
724   explains interannual and seasonal variation in carbon and water exchange in a semiarid mature
725   ponderosa pine forest in central Oregon, Journal of Geophysical Research: Biogeosciences (2005–2012),
726   114, 2009.
727   Van Tuyl, S., Law, B., Turner, D., and Gitelman, A.: Variability in net primary production and carbon
728   storage in biomass across Oregon forests—an assessment integrating data from forest inventories,
729   intensive sites, and remote sensing, Forest Ecology and Management, 209, 273-291, 2005.
730   Walsh, J., Wuebbles, D., Hayhoe, K., Kossin, J., Kunkel, K., Stephens, G., Thorne, P., Vose, R., Wehner, M.,
731   Willis, J., Anderson, D., Doney, S., Feely, R., Hennon, P., Kharin, V., Knutson, T., Landerer, F., Lenton, T.,
732   Kennedy, J., and Somerville, R.: Our Changing Climate, in: Climate Change Impacts in the United States:
733   The Third National Climate Assessment, edited by: Melillo, J. M., Richmond, T. C., and Yohe, G. W., U.S.
734   Global Change Research Program, 19-67, 2014.
735   Waring, R.: Estimating forest growth and efficiency in relation to canopy leaf area, Adv. Ecol. Res, 13,
736   327-354, 1983.
737   Waring, R. H., and Franklin, J. F.: Evergreen coniferous forests of the Pacific Northwest, Science, 204,
738   1380-1386, 1979.
739   Waring, R. H., and Running, S. W.: Forest Ecosystems: Analysis at Multiple Scales, 3rd ed., Elsevier
740   Academic Press, Burlington, MA, 420 pp., 2007.
741   Webb, W. L., Lauenroth, W. K., Szarek, S. R., and Kinerson, R. S.: Primary production and abiotic controls
742   in forests, grasslands, and desert ecosystems in the United States, Ecology, 134-151, 1983.
743   Whittaker, R. H.: Estimation of net primary production of forest and shrub communities, Ecology, 42,
744   177-180, 1961.
745   Whittaker, R. H., and Niering, W. A.: Vegetation of the Santa Catalina Mountains, Arizona. V. Biomass,
746   production, and diversity along the elevation gradient, Ecology, 56, 771-790, 1975.
747   Wickham, H., and Francois, R.: dplyr: A Grammar of Data Manipulation, R package version 0.4.2,
748   http://CRAN.R-project.org/package=dplyr, 2015.
749   Wilcox, K. R., Blair, J. M., Smith, M. D., and Knapp, A. K.: Does ecosystem sensitivity to precipitation at
750   the site-level conform to regional-scale predictions?, Ecology, 97, 561-568, 2016.

751 Williams, A. P., Seager, R., Macalady, A. K., Berkelhammer, M., Crimmins, M. A., Swetnam, T. W.,
752 Trugman, A. T., Buenning, N., Noone, D., and McDowell, N. G.: Correlations between components of the
753 water balance and burned area reveal new insights for predicting forest fire area in the southwest
754 United States, International Journal of Wildland Fire, 24, 14-26, 10.1071/WF14023, 2014.
755 Williams, M., Rastetter, E., Fernandes, D., Goulden, M., Wofsy, S., Shaver, G., Melillo, J., Munger, J., Fan,
756 S. M., and Nadelhoffer, K.: Modelling the soil-plant-atmosphere continuum in a Quercus–Acer stand at
757 Harvard Forest: the regulation of stomatal conductance by light, nitrogen and soil/plant hydraulic
758 properties, Plant, Cell & Environment, 19, 911-927, 1996.
759 Williams, M.: Deforesting the Earth: From Prehistory to Global Crisis, University of Chicago Press,
760 Chicago, USA, 543 pp., 2006.
761 Wilson, B. T., Woodall, C., and Griffith, D.: Imputing forest carbon stock estimates from inventory plots
762 to a nationally continuous coverage, Carbon balance and management, 8, 1, 2013.
763 Yan, K., Park, T., Yan, G., Liu, Z., Yang, B., Chen, C., Nemani, R. R., Knyazikhin, Y., and Myneni, R. B.:
764 Evaluation of MODIS LAI/FPAR Product Collection 6. Part 2: Validation and Intercomparison, Remote
765 Sensing, 8, 460, 2016.
766 Yang, Y., Fang, J., Ma, W., and Wang, W.: Relationship between variability in aboveground net primary
767 production and precipitation in global grasslands, Geophysical Research Letters, 35, 2008.
768 Zhao, M., Running, S., Heinsch, F. A., and Nemani, R.: MODIS-derived terrestrial primary production, in:
769 Land Remote Sensing and Global Environmental Change: NASA's Earth Observing System and the
770 Science of ASTER and MODIS, edited by: Ramachandra, B., Justice, C. O., and Abrams, M. J., Springer,
771 New York, 635-660, 2010.
772 Zotarelli, L., Dukes, M. D., Romero, C. C., Migliaccio, K. W., and Morgan, K. T.: Step by step calculation of
773 the Penman-Monteith Evapotranspiration (FAO-56 Method), Institute of Food and Agricultural Sciences.
774 University of Florida, 2010.

775

776

777

778

779

780

781

782

783

784

785

786 **Tables**

787 Table 1. Summary of tree net primary productivity (NPP; Mg C ha^{-1} yr^{-1}), live biomass (BIO; Mg C ha^{-1}),

788 and carbon residence time (CRT; year) for stands over 100 years old across both WAORCA and the

789 broader western US. These forest characteristics were quantified for WAORCA using field measurements

790 from 1,953 sites and for the western US using satellite-derived data sets covering 18 Mha of mature

791 forest. Satellite data sets included MODIS NPP and an estimate of BIO derived by combining existing

792 maps of aboveground biomass with additional estimates of carbon storage in coarse root, fine roots, and

793 foliage. These carbon stocks and fluxes combine above- and below-ground components.

Domain	Variable	Units	Time span	Mean (SD)	Range
WAORCA	NPP_{field}	Mg C ha^{-1} yr^{-1}	2001-2006	4.3 (2.5)	0.6 – 20.9
	BIO_{field}	Mg C ha^{-1}	2001-2006	158 (135)	2 – 947
	CRT_{field}	year	2001-2006	33 (19)	2 – 137
Western US	NPP_{sat}	Mg C ha^{-1} yr^{-1}	2000-2014	5.3 (2.0)	0.1 – 227
	BIO_{sat}	Mg C ha^{-1}	2000-2008	83 (54)	2 – 669
	CRT_{sat}	year	2000-2008	15 (9)	2 – 1390

794

795

796

797

798

799

800

801

802

803

804

805

806   Table 2. Changes in tree net primary productivity (NPP; Mg C ha^{-1} yr^{-1}), live biomass (BIO; Mg

807   C ha^{-1}), and carbon residence time (CRT; year) for stands over 100 years old along gradients in a

808   climate moisture index (CMI$_{\overline{wy}}$; cm yr^{-1}) in both WAORCA and the broader western US. Forest

809   characteristics were quantified using field measurements in WAORCA and satellite remote

810   sensing data sets covering the western US. The analysis incorporated forests in areas where

811   CMI$_{\overline{wy}}$ was between -200 cm yr^{-1} and 200 cm yr^{-1}. Summaries include (1) median forest

812   characteristic in the driest 5% and wettest 95% of sites/pixels; (2) the corresponding change; (3)

813   and Spearman's correlation (r$_s$) between CMI$_{\overline{wy}}$ and the median forest characteristic computed at

814   10 cm yr^{-1} CMI$_{\overline{wy}}$ intervals. All correlations were statistically significant at $\alpha < 0.001$.

Domain	Variable	Units	Median of…		Change…		CMI$_{\overline{wy}}$ cor.
			Driest 5%	Wettest 95%	Abs.	%	r$_s$
WAORCA	NPP$_{field}$	Mg C ha^{-1} yr^{-1}	2.2	5.6	3.4	155	0.93
	BIO$_{field}$	Mg C ha^{-1}	26	281	255	997	0.96
	CRT$_{field}$	year	11	49	38	358	0.96
Western US	NPP$_{sat}$	Mg C ha^{-1} yr^{-1}	3.4	6.7	3.3	97	0.93
	BIO$_{sat}$	Mg C ha^{-1}	32	165	133	410	0.97
	CRT$_{sat}$	year	10	26	16	160	0.99

815

816

817

818

819

820

821

822

823

824

825

826 **Figures**

827
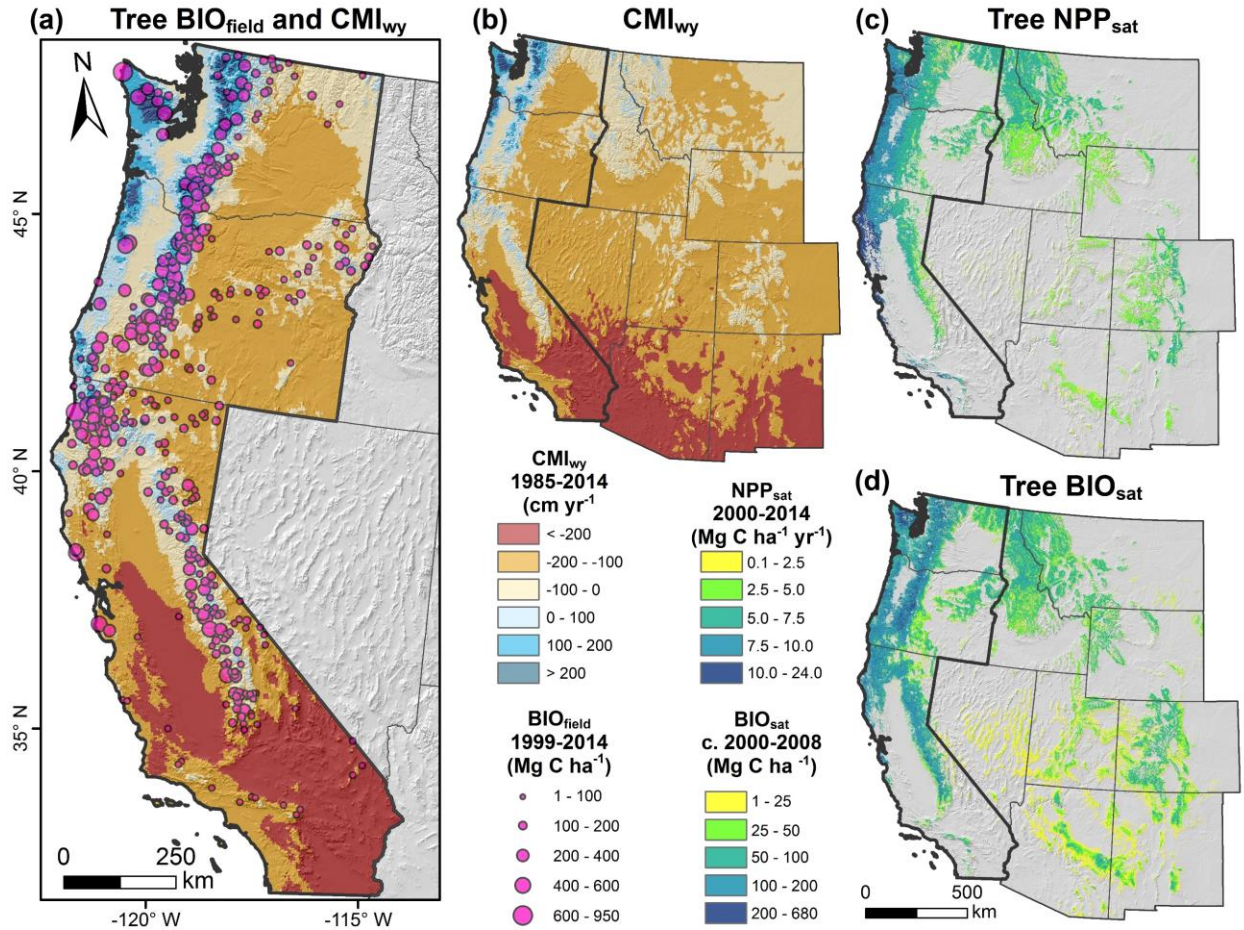
828 Figure 1. Mean climatic moisture index (CMI$_{\overline{wy}}$; cm yr^{-1}), tree net primary productivity (NPP;

829 Mg C ha^{-1} yr^{-1}), and live tree biomass (BIO; Mg C ha^{-1}) in the western US. (a) BIO derived from

830 field measurements (BIO$_{field}$) at mature sites (>100 years) in WAORCA. For visual clarity only

831 20% of the 1,953 sites are depicted. (b) CMI$_{\overline{wy}}$ was computed as monthly precipitation minus

832 reference evapotranspiration summed over the annual water year (October-September) and then

833 averaged from 1985-2014. (c) Mean annual NPP was quantified using MODIS satellite data from

834 2000-2014 (NPP$_{sat}$). (d) BIO was quantified using satellite-derived estimates of carbon stocks

835 (BIO$_{sat}$).

836

837

838
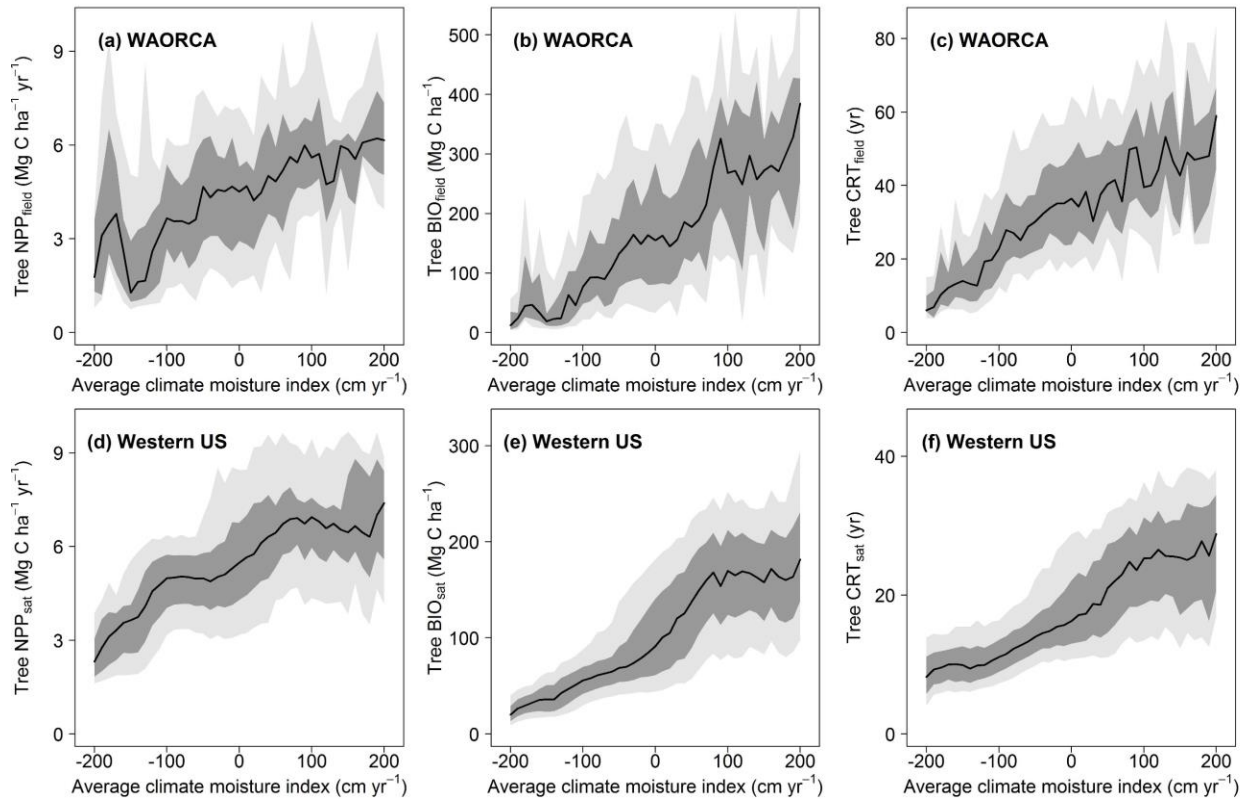
Figure 2. Tree net primary productivity (NPP; Mg C ha^{-1} yr^{-1}), live biomass (BIO; Mg C ha^{-1}),

and carbon residence time (CRT; years) increased with increasing water availability across both

WAORCA (a-c) and the broader western US (d-f). Forest characteristics were derived from field

measurements on 1,953 inventory plots in WAORCA (a-c) and from satellite remote sensing

data sets across 18 Mha of mature forest in the western US (d-f). NPP_{sat} was characterized using

MODIS data averaged annually from 2000 to 2014. BIO_{sat} was quantified based on an ensemble

of aboveground biomass maps plus estimates of coarse root, fine root, and foliage biomass. CRT

was computed for each field plot and pixel as BIO / NPP. Water availability was quantified using

a climate moisture index ($CMI = P-ET_0$) summed over the water year (October-September) and

then averaged from 1985-2014 ($CMI_{\overline{wy}}$). The region was partitioned into 10 cm yr^{-1} (non-

849 overlapping) $CMI_{\overline{wy}}$ bins, pixels/plots were allocated to bins, and then forest characteristics were

850 summarized within each bin. In each panel, the bold line denotes the median, dark gray band the

851 25-75th percentiles, and light gray band the 10-90th percentiles. Note the different y-axis scales

852 between (b) and (e), as well as (c) and (f).